

FRET-Enabled Optical Modulation for High Sensitivity Fluorescence Imaging

Chris I. Richards, Jung-Cheng Hsiang, Andrew M. Khalil, Nathan P. Hull, and Robert M. Dickson*

School of Chemistry and Biochemistry and Petit Institute for Biosciences and Bioengineering, Georgia Institute of Technology, Atlanta, Georgia 30332-0400

Received September 18, 2009; Revised Manuscript Received January 8, 2010; E-mail: dickson@chemistry.gatech.edu

Abstract: Fluorescence resonance energy transfer is utilized to engineer donor photophysics for facile signal amplification and selective fluorescence recovery from high background. This is generalized such that many different fluorophores can be used in optical modulation schemes to drastically improve fluorescence imaging sensitivity. Dynamic, simultaneous, and direct excitation of the acceptor brightens and optically modulates higher energy donor emission. The externally imposed modulation waveform enables selective donor fluorescence extraction through demodulation. By incorporating an acceptor with significant, spectrally shifted, dark-state population, necessary excitation intensities are quite low and agree well with simulated enhancements. Enhancement versus modulation frequency directly yields dark-state lifetimes in a simple ensemble measurement. Using the long-lived Cy5 dark state in conjunction with Cy3 donors, we demonstrate image extraction from a large background to yield $\gg 10$ -fold sensitivity improvements through synchronously amplified fluorescence image recovery (SAFIRE).

Introduction

Fluorescent imaging is often plagued by high background that obscures signals of interest,^{1,2} commonly limiting both intracellular^{3,4} and deep tissue applications.^{5–7} Recently, saturated^{8,9} or stimulated transitions,^{10,11} structured light illumination,^{12,13} and reversible fluorophore photobleaching^{5,6,14–17} have enabled signal modulation and recovery schemes to be adapted to

fluorescence imaging, resulting in resolution and sensitivity gains. In parallel, we demonstrated a more dynamic and lower background modulation scheme by optically reversing transient blinking in engineered fluorophores through long-wavelength depopulation of Ag nanodot dark states.¹⁸ In contrast to reversible but thermally stable and high-energy absorbing photoswitches,¹⁴ modulated optical depopulation of trap states through coillumination at wavelengths longer than that of the collected fluorescence enables more dynamic synchronously amplified fluorescence image recovery (SAFIRE), and a more general and higher sensitivity dynamic route to fluorescent signal recovery.¹⁹ Because the modulated secondary laser excitation is lower energy than is the collected fluorescence, only the signal of interest is modulated, independent of background. Further, signals are directly extracted via Fourier transform-based demodulation of the known, externally applied modulation waveform, such that exogenously incorporated internal standards for waveform elucidation^{14,16} are unnecessary.^{18,19} Although dynamic dark-state optical depopulation has distinct signal recovery advantages, fluorescent systems must have inherent transitions into dark states that can be manipulated at wavelengths longer than that of the emitted fluorescence, limiting the pool of useful fluorophores.¹⁹ For such systems with long-wavelength transient absorptions leading to photoinduced dark-state decay, lower energy secondary coexcitation enables increased fluorophore emission without increasing background fluorescence. Further, while such transitions may enable sen-

- (1) Tokunaga, M.; Imamoto, N.; Sakata-Sogawa, K. *Nat. Methods* **2008**, *5*, 455–455.
- (2) Sako, Y.; Minoguchi, S.; Yanagida, T. *Nat. Cell Biol.* **2000**, *2*, 168–172.
- (3) Elf, J.; Li, G. W.; Xie, X. S. *Science* **2007**, *316*, 1191–1194.
- (4) Kural, C.; Kim, H.; Syed, S.; Goshima, G.; Gelfand, V. I.; Selvin, P. R. *Science* **2005**, *308*, 1469–1472.
- (5) Bates, M.; Huang, B.; Dempsey, G. T.; Zhuang, X. *Science* **2007**, *317*, 1749–1753.
- (6) Betzig, E.; Patterson, G. H.; Sougrat, R.; Lindwasser, O. W.; Olenych, S.; Bonifacino, J. S.; Davidson, M. W.; Lippincott-Schwartz, J.; Hess, H. F. *Science* **2006**, *313*, 1642–1645.
- (7) Bossi, M.; Below, V.; Polyakova, S.; Hell, S. W. *Angew. Chem., Int. Ed.* **2006**, *45*, 7462–7465.
- (8) Hell, S. W.; Kroug, M. *Appl. Phys. B* **1995**, *60*, 495–497.
- (9) Fujita, K.; Kobayashi, M.; Kawano, S.; Yamanaka, M.; Kawata, S. *Phys. Rev. Lett.* **2007**, *99*, 228105.
- (10) Hell, S. W. *Science* **2007**, *316*, 1153–1158.
- (11) Hell, S. W.; Wichmann, J. *Opt. Lett.* **1994**, *19*, 780–782.
- (12) Gustafsson, M. G. L. *J. Microsc. (Oxford, U.K.)* **2000**, *198*, 82–87.
- (13) Hirvonen, L. M.; Wicker, K.; Mandula, O.; Heintzmann, R. *Eur. Biophys. J. Biophys. Lett.* **2009**, *38*, 807–812.
- (14) Marriott, G.; Mao, S.; Sakata, T.; Ran, J.; Jackson, D. K.; Petchprayoon, C.; Gomez, T. J.; Warp, E.; Tulyathan, O.; Aaron, H. L.; Isacoff, E. Y.; Yan, Y. *Proc. Natl. Acad. Sci. U.S.A.* **2008**, *105*, 17789–17794.
- (15) Hess, S. T.; Girirajan, T. P. K.; Mason, M. D. *Biophys. J.* **2006**, *91*, 4258–4272.
- (16) Mao, S.; Benninger, R. K. P.; Yan, Y. L.; Petchprayoon, C.; Jackson, D.; Easley, C. J.; Piston, D. W.; Marriott, G. *Biophys. J.* **2008**, *94*, 4515–4524.

- (17) Biteen, Julie S.; T., M. A.; Tselentis, Nicole K.; Bowman, Grant R.; Shapiro, Lucy; Moerner, W E. *Nat. Methods* **2008**, *5*, 947–949.
- (18) Richards, C. I.; Hsiang, J.-C.; Senapati, D.; Patel, S.; Yu, J.; Vosch, T.; Dickson, R. M. *J. Am. Chem. Soc.* **2009**, *131*, 4619–4621.
- (19) Richards, C. I.; Hsiang, J.-C.; Dickson, R. M. *J. Phys. Chem. B* **2010**, *114*, 660–665.

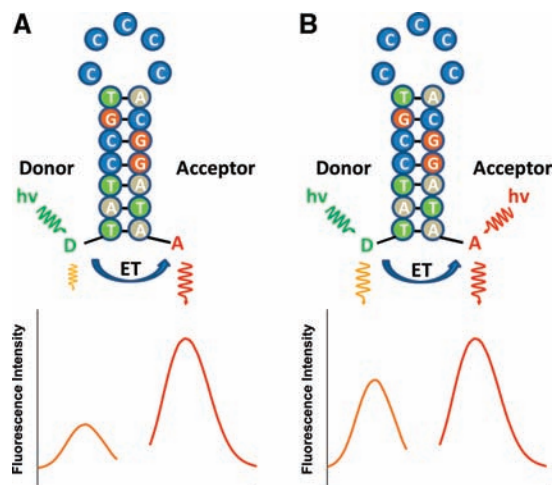


Figure 1. Schematic of a 19-base hairpin exhibiting FRET with donor and acceptor fluorophores. (A) Typical FRET process when only the donor is excited, leading to highly quenched donor fluorescence. (B) Inhibited FRET and increased donor fluorescence quantum yield resulting from simultaneous acceptor direct excitation that inhibits FRET through creating a higher steady-state acceptor excited-state population (with spectrally shifted absorption), thereby increasing and enabling modulation of donor fluorescence.

sitivity increases via demodulation, the required dark-state transitions may limit fluorophore brightness by decreasing fluorescence quantum yield and sustainable emission rates. While SAFIRE advantageously utilizes dark-state transitions to improve imaging sensitivity,¹⁹ blinking behavior remains detrimental to most imaging applications,^{20–23} with poorly defined and controlled transient trap states^{24–27} still limiting most applications.

Circumventing the need for long dark-state residence and long-wavelength dark-state transient absorption, we build on the concept of acceptor saturation (satFRET) for FRET efficiency measurements^{28–31} to generalize the modulation and specific detection of a wide array of donor fluorophores. Combining any fluorophore as the donor in a FRET pair quenches its emission while simultaneously providing an opportunity for longer-than-donor-fluorescence-wavelength excitation to coexcite the acceptor. As schematized in Figure 1A,

donor excitation alone results in efficient energy transfer, thereby quenching donor emission. Simultaneous acceptor excitation at wavelengths longer than much of the donor emission, however, inhibits FRET-based quenching to dynamically increase donor fluorescence quantum yield. This general enhancement scheme is shown in Figure 1B and results from a shift of the acceptor excited-state absorption relative to that in the ground state, thereby decreasing the rate of FRET from the excited donor relative to the rate of fluorescence. Such FRET rate decreases will result when the acceptor excited-state absorption spectrum exhibits limited overlap with the donor emission, reducing the dipole–dipole coupling between donor and excited acceptor as compared to the acceptor ground state. Herein we implement and demonstrate the utility of this concept, showing that such direct acceptor excitation (and modulation of the secondary excitation source) dynamically decreases the FRET rate to simultaneously increase the donor fluorescence quantum yield. Demodulation recovers only those species whose FRET is modulated, selectively recovering desired fluorophore signals from high backgrounds. This provides a new, general, and selective fluorescence amplification scheme applicable to fluorescent image recovery in high background environments. In contrast to optically enhancing fluorophore emission by optically exciting brightness-limiting, long-lived, moderate-yield dark states,¹⁹ FRET is nearly ideal for synchronous amplification of target fluorescence, giving both significant enhancement and modulation depth with excellent brightness and dynamic range.

Experimental Methods

Fluorescently labeled DNA hairpin-forming oligonucleotides (5'-TAT CCG TCC CCC ACG GAT A-3', with either 6-Fam (6-carboxyfluorescein) and TAMRA (tetramethylrhodamine) or Cy3 and Cy5 attached to the 3' and 5' ends, respectively) were obtained from Integrated DNA Technology (IDT) and were prepared by dissolving in deionized water (18 M Ω). Donor-only labeled hairpins were also obtained and studied as controls. Hairpin formation was optimized by heating to 70 °C for 15 min followed by cooling to room temperature. FRET hairpin solutions were studied on a microscope (Olympus IX 71) using a 60X water-immersion objective (Olympus 1.2 NA). Image stacks were collected with an EM-CCD (Andor Ixon 897) at frame rates synchronized to but 10 times faster than the modulation frequency. Fourier transforms of the resulting time traces from each pixel versus time were used to extract the modulation frequency component. The corresponding Fourier amplitude at the modulation frequency of each pixel was used to recover the demodulated image. Intensity trajectories were collected in a confocal arrangement using a multimode fiber as a pinhole. The emission was detected with an avalanche photodiode (Perkin-Elmer) and recorded using a Becker-Hickl photon counting module (SPC 630). Appropriate band-pass filters centered near the emission wavelength of the specific dye were used to efficiently block both the primary excitation and the lower energy secondary laser excitation. Continuous wave primary laser excitation was used near the typical excitation maximum of the dye using a tunable Ar⁺ laser (Coherent). A 561 nm solid state (Coherent) or 633 nm helium neon (Spectra Physics) laser was used as the secondary excitation for TAMRA or Cy5, respectively. For experiments utilizing dual-laser excitation, lasers were overlapped using a dichroic mirror prior to entering the microscope and at the sample plane. Modulation of the secondary laser was performed with a mechanical chopper (Stanford Research Systems).

Corresponding to the known and measured photophysics of the 6-Fam-TAMRA^{32–35} and Cy3-Cy5^{36–39} systems with FRET-

- (20) Vogelsang, J.; Cordes, T.; Forthmann, C.; Steinhauer, C.; Tinnefeld, P. *Proc. Natl. Acad. Sci. U.S.A.* **2009**, *106*, 8107–8112.
- (21) Steinhauer, C.; Forthmann, C.; Vogelsang, J.; Tinnefeld, P. *J. Am. Chem. Soc.* **2008**, *130*, 16840–16841.
- (22) Cordes, T.; Vogelsang, J.; Tinnefeld, P. *J. Am. Chem. Soc.* **2009**, *131*, 5018–5019.
- (23) Vogelsang, J.; Kasper, R.; Steinhauer, C.; Person, B.; Heilemann, M.; Sauer, M.; Tinnefeld, P. *Angew. Chem., Int. Ed.* **2008**, *47*, 5465–5469.
- (24) Clifford, J. N.; Bell, T. D. M.; Tinnefeld, P.; Heilemann, M.; Melnikov, S. M.; Hotta, J.; Sliwa, M.; Dedecker, P.; Sauer, M.; Hofkens, J.; Yeow, E. K. L. *J. Phys. Chem. B* **2007**, *111*, 6987–6991.
- (25) Dickson, R. M.; Cubitt, A. B.; Tsien, R. Y.; Moerner, W. E. *Nature* **1997**, *388*, 355–358.
- (26) Yip, W. T.; Hu, D. H.; Yu, J.; Vanden Bout, D. A.; Barbara, P. F. *J. Phys. Chem. A* **1998**, *102*, 7564–7575.
- (27) Wang, S.; Querner, C.; Emmons, T.; Drndic, M.; Crouch, C. H. *J. Phys. Chem. B* **2006**, *110*, 23221–23227.
- (28) Schonle, A.; Hanninen, P. E.; Hell, S. W. *Ann. Phys. (Berlin, Ger.)* **1999**, *8*, 115–133.
- (29) Hanninen, P. E.; Lehtela, L.; Hell, S. W. *Opt. Commun.* **1996**, *130*, 29–33.
- (30) Beutler, M.; Makrogianneli, K.; Vermeij, R. J.; Keppler, M.; Ng, T.; Jovin, T. M.; Heintzmann, R. *Eur. Biophys. J. Biophys. Lett.* **2008**, *38*, 69–82.
- (31) Jares-Erijman, E. A.; Jovin, T. M. *Nat. Biotechnol.* **2003**, *21*, 1387–1395.

- (32) Banishev, A. A.; Maslov, D. V.; Fadeev, V. V. *Vestn. Mosk. Univ. Fiz.* **2008**, *63*, 218–220.

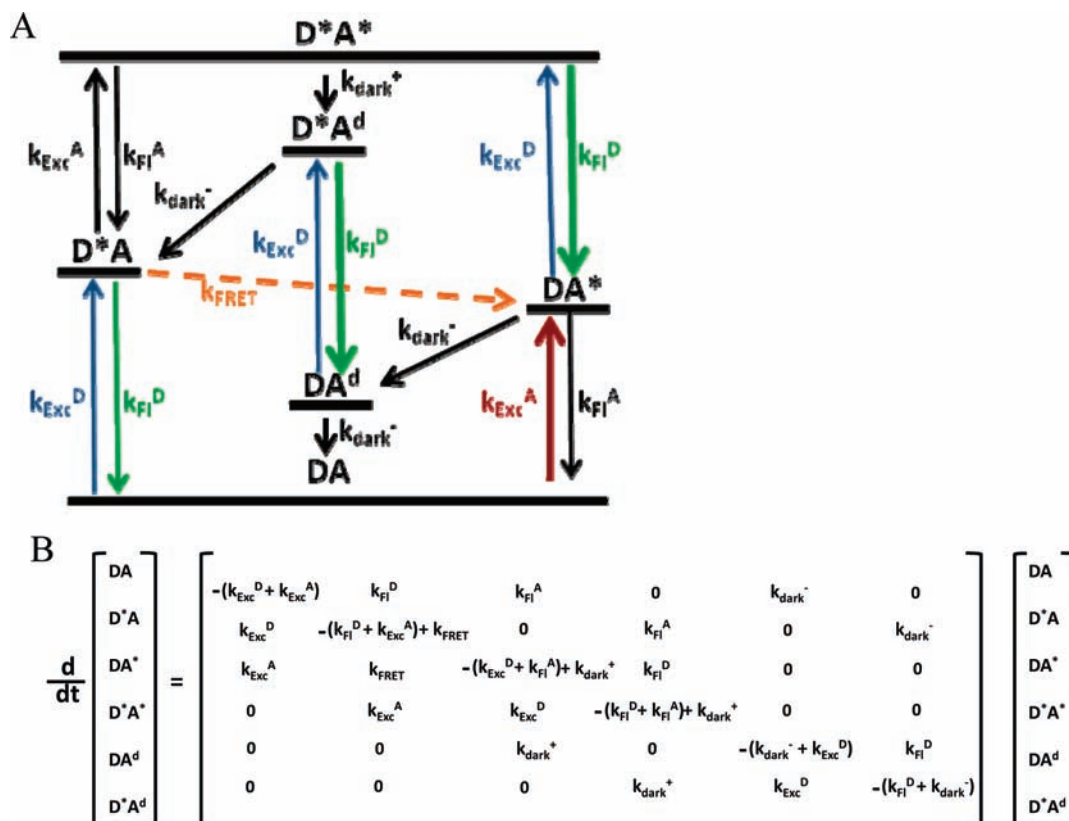


Figure 2. (A) Schematic model enabling donor fluorescence enhancement and modulation through dual laser excitation. Bold arrows show the transitions giving enhanced fluorescence. The arrow connecting D^*A^d to DA^d is the primary enhancement pathway in the Cy3–Cy5 system, whereas the D^*A^* to DA^* transition also contributes significantly to the enhanced emission for 6-Fam–TAMRA, when no long-lived dark state is present. (B) Rate equations corresponding to population and depopulation of all 6 levels as diagrammed in Figure 2A. The photophysical parameters used for determining transitions between states for Cy3–Cy5^{36–39} were $\lambda_D = 496$ nm, $\lambda_A = 633$ nm, $\Phi_{dark} = 0.0003$, $\tau_D = 3.5$ ns, $\tau_A = 3.0$ ns, $E_{FRET} = 0.47$, $\tau_{dark^-} = 500$ μ s, $\epsilon_D(496$ nm) = 30,000 M⁻¹ cm⁻¹, $\epsilon_A(633$ nm) = 250,000 M⁻¹ cm⁻¹. The photophysical parameters used for determining transitions between states for 6-Fam–TAMRA^{32–35} were $\lambda_D = 476$ nm, $\lambda_A = 561$ nm, $\Phi_{dark} = 0.001$, $\tau_D = 3.5$ ns, $\tau_A = 3.0$ ns, $E_{FRET} = 0.90$, $\tau_{dark^-} = 10$ μ s, $\epsilon_D(476$ nm) = 60,000 M⁻¹ cm⁻¹, $\epsilon_A(561$ nm) = 50,000 M⁻¹ cm⁻¹.

coupled excited states, a 6-level model was constructed depicting the relevant states (Figure 2A). Rates for excitation and relaxation combined with dark-state transitions were utilized to yield steady-state populations of all levels when illuminated with known primary and secondary excitation intensities. Included in the model are donor ground (D) and excited (D^*) states, as well as acceptor ground (A), excited (A^*), and dark states (A^d). Subscripts Exc and Fl denote excitation and fluorescence, respectively. Solving the set of differential equations governing transitions among states yields the relative time-dependent populations (Figure 2B). Excitation rates are defined as simply absorption cross section (σ) multiplied by the excitation intensity (I), and fluorescence rates are determined by the inverse of the fluorescence lifetime. Steady-state populations under donor excitation alone and with simultaneous direct excitation of the acceptor are readily calculated. Sequential exposure to the secondary excitation at varying frequencies was used to calculate

the dependence of the enhancement on the modulation frequency. If long-lived dark states are present, high modulation frequencies provide insufficient time for steady-state populations to be established, thereby limiting modulation depth at higher frequencies. In all cases, enhancement (i.e., modulation depth) is determined by the ratio of fluorescence under dual laser illumination to that with primary illumination alone. Acceptor saturation increases the donor fluorescence quantum yield by inhibiting (slowing down) the rate of FRET.

Results and Discussion

To demonstrate donor fluorescence enhancement, we utilized the hairpin with 6-Fam (6-carboxyfluorescein) on the 5' end and TAMRA (tetramethylrhodamine) on the 3' end. 6-Fam on this oligo strand without the TAMRA exhibits no modulation upon 561 nm coillumination at any of the intensities investigated. Attaching TAMRA to the 3' end, however, yields moderate 6-Fam fluorescence enhancement upon concurrent direct laser excitation of the acceptor (Figure 3A). FRET inhibition relies on the acceptor excited state being occupied for a significant percentage of donor excitation cycles and any acceptor transient absorption being significantly shifted away from that of the ground state absorption. Consequently, as with satFRET-based efficiency measurements,^{28–31} modeling simple steady-state populations of the FRET-coupled dyes suggests that very high continuous wave excitation intensities are needed to reach even moderate enhancements from low steady-state

- (33) Neubauer, H.; Gaiko, N.; Berger, S.; Schaffer, J.; Eggeling, C.; Tuma, J.; Verdier, L.; Seidel, C. A. M.; Griesinger, C.; Volkmer, A. *J. Am. Chem. Soc.* **2007**, *129*, 12746–12755.
- (34) Yamashita, M.; Kuniyasu, A.; Kashiwagi, H. *J. Chem. Phys.* **1977**, *66*, 986–988.
- (35) Ferguson, M. W.; Beaumont, P. C.; Jones, S. E.; Navaratnam, S.; Parsons, B. J. *J. Phys. Chem. Phys.* **1999**, *1*, 261–268.
- (36) Tinnefeld, P.; Buschmann, V.; Weston, K. D.; Sauer, M. J. *J. Phys. Chem. A* **2003**, *107*, 323–327.
- (37) Huang, Z. X.; Ji, D. M.; Wang, S. F.; Xia, A. D.; Koberling, F.; Patting, M.; Erdmann, R. *J. Phys. Chem. A* **2006**, *110*, 45–50.
- (38) Jia, K.; Wan, Y.; Xia, A. D.; Li, S. Y.; Gong, F. B.; Yang, G. Q. *J. Phys. Chem. A* **2007**, *111*, 1593–1597.
- (39) Widengren, J.; Schwille, P. *J. Phys. Chem. A* **2000**, *104*, 6416–6428.

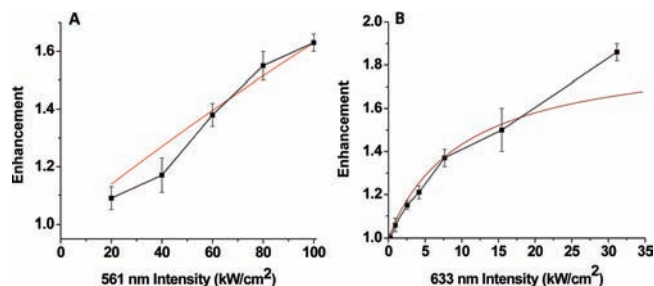


Figure 3. (A) Predicted enhancement of a 6-Fam-TAMRA-labeled hairpin undergoing FRET (E_{FRET} measured at $\sim 90\%$) with constant cw 476 nm (10 kW/cm^2) excitation and varied cw 561 nm intensity using a dark-state quantum yield of 10^{-3} and dark-state lifetime of $10 \mu\text{s}$. Measured enhancement from a 125 nM aqueous solution (■) with 476 nm (10 kW/cm^2) and varied 561 nm secondary excitation. (B) Predicted enhancement (red) of a Cy3-Cy5 hairpin exhibiting FRET ($E_{\text{FRET}} \approx 47\%$) with constant cw 496 nm (1 kW/cm^2) excitation and varied cw 633 nm intensity using an acceptor dark-state quantum yield of 3×10^{-4} and dark-state lifetime of $500 \mu\text{s}$.³⁷ (■) Measured enhancement with constant 496 nm (1 kW/cm^2) excitation and varied cw 633 nm secondary intensity. Maximum expected enhancements are given by $(1 - E_{\text{FRET}})^{-1}$, suggesting values of 10 and 2 for the systems in A and B, respectively.

acceptor excited-state occupation (Figure 3A, red curve). Calculated enhancements were performed at the same constant primary (10 kW/cm^2) and varied secondary laser intensities used in the experiments. The resulting calculated enhancement is plotted with the experimental data. At these high laser intensities, the reported photophysical parameters for 6-Fam and TAMRA incorporated in our model clearly predict donor fluorescence enhancement to reach $\sim 60\%$ as the secondary excitation intensity reaches 100 kW/cm^2 . Just over a quarter of the enhancement would arise from singlet saturation, with the other three-quarters arising from the steady-state population of the $\sim 10\text{-}\mu\text{s}$ -lived⁴⁰ dark state. Although the transient absorption of TAMRA has not, to our knowledge, been reported, studies on various rhodamines suggest that excited-state absorption shifts very far to the blue,^{35,41,42} which would preclude the rhodamine excited state from acting as a FRET acceptor, thereby providing the necessary modulation of donor emission. Measured enhancement values at varied 561 nm excitation nicely mirror the predicted intensity-dependent enhancements (Figure 3A). These observations, coupled with the excellent agreement with the rate-based model of FRET inhibition using only experimentally determined values,^{32–34} clearly demonstrate that donor fluorescence enhancement results from significant steady-state excited acceptor populations (Figure 3A). Any spectral shift or decrease in acceptor absorption cross section resulting from excited-state occupation is likely to reduce FRET rates relative to those with optimized acceptor ground state overlap with donor emission ($\sim 90\%$ for 6-Fam-TAMRA). Therefore, rapid optical modulation of this emission should also occur when a significant steady-state acceptor excited-state population difference is achieved for single- versus dual-laser excitation.

As population of the acceptor excited state transiently shifts acceptor absorption to most likely decrease spectral overlap with donor emission from that optimized for ground state overlap, FRET is inhibited. Therefore, increasing the excited steady-state population of the acceptor should further significantly

increase enhancement. Consequently, to generate enhancement at more modest excitation intensities, we replaced 6-Fam and TAMRA with Cy3 and Cy5, respectively. Cyanine dyes and Cy5 in particular are well-known to have long-lived dark states with complicated photophysics arising from both a nonfluorescent isomer and an energy-transfer-accepting triplet state.^{36–39,43} Transient absorption studies demonstrate that triplet–triplet absorption (625 nm max) has significant spectral overlap with the primary ground state singlet–singlet excitation (647 nm), while the longer-lived nonfluorescent isomer absorption is significantly red-shifted (690 nm).³⁷ The similar triplet absorption spectrum enables this short-lived ($\sim 10 \mu\text{s}$) state to act effectively as a nonradiative acceptor of energy transfer from the donor. The longer-lived ($\sim 500 \mu\text{s}$) cis Cy5 dark state, however, is also formed in high yield but exhibits a stronger and significantly red-shifted transient absorption that drastically slows energy transfer due to poor spectral overlap with donor emission. It is the steady-state occupation of this state that we use to actually inhibit FRET at low excitation intensities.^{38,43,44} Governed by the high yield and long lifetime of the cis isomer, dual-laser excitation (496 nm primary, 633 nm secondary) of the Cy3-Cy5-labeled hairpin within a $1 \mu\text{M}$ aqueous solution (Figure 3B), yields similar enhancements to those of 6-FAM-TAMRA pairs, but at an order of magnitude lower primary and secondary excitation intensities (Figure 3). Maximum enhancements of Cy3-Cy5 easily approach 90%, again at relatively low excitation intensities (1 kW/cm^2 primary, 30 kW/cm^2 secondary). As with the 6-Fam-TAMRA system, no Cy3 enhancement is observed without the Cy5 acceptor simultaneously being present. The low intensities at which significant enhancement is observed suggests a large steady-state population of the well-known, long-lived Cy5 dark state.³⁷ Incorporating a few hundred microsecond-lived FRET-inhibiting acceptor dark state^{37,45} into the rate model yields a large steady-state dark-state population that faithfully models the observed low-intensity Cy3 fluorescence enhancement (Figure 3B). Using the known Cy5 triplet lifetime ($\sim 3 \mu\text{s}$),³⁹ however, does not yield significant enhancements at these excitation intensities. Further, in contrast to most single molecule experiments, the steady-state triplet population in our fully aerated solutions is much lower than that of the longer-lived spectrally shifted cis-Cy5 isomer.³⁷ The strong agreement between the model and the experimental data demonstrates that the long dark-state residence greatly increases the probability of simultaneous excited-state population, thereby enhancing Cy3 emission at very low secondary excitation intensities via FRET inhibition.

Although clearly a FRET-inhibiting steady-state buildup of excited-state dark-state population occurs, sensitivity gains require the rapid establishment of different steady-state populations under fast switching between single and dual laser illumination. Such synchronously amplified fluorescence image recovery (SAFIRE)^{18,19} would then enable encoding the fluorescence with the externally applied modulating waveform. Although the high, steady-state acceptor excited-state population enables low incident laser intensities for high contrast fluorescence modulation, the long-lived dark-state decay should also limit attainable modulation frequencies. In fact, the frequency-

(40) Kinjo, M.; Rigler, R. *Nucleic Acid Res.* **1995**, *23*, 1795–9.

(41) Dobryakov, A. L.; Kovalenko, S. A.; Ernstring, N. P. *J. Chem. Phys.* **2005**, *123*.

(42) Beaumont, P. C.; Johnson, D. G.; Parsons, P. J. *J. Photochem. Photobiol., A* **1997**, *107*, 175–183.

(43) Heilemann, M.; Margeat, E.; Kasper, R.; Sauer, M.; Tinnefeld, P. *J. Am. Chem. Soc.* **2005**, *127*, 3801–3806.

(44) Buschmann, V.; Weston, K. D.; Sauer, M. *Bioconjugate Chem.* **2003**, *14*, 195–204.

(45) White, S. S.; Li, H. T.; Marsh, R. J.; Piper, J. D.; Leonczek, N. D.; Nicolaou, N.; Bain, A. J.; Ying, L. M.; Klenerman, D. *J. Am. Chem. Soc.* **2006**, *128*, 11423–11432.

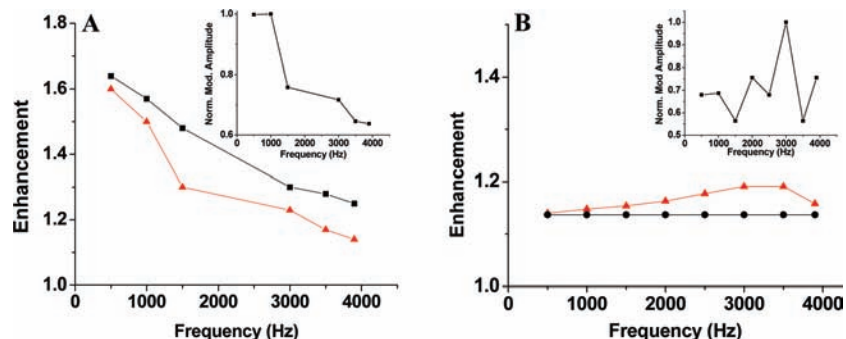


Figure 4. (A) Cy3 fluorescence enhancement within the Cy3-Cy5 hairpin ($1 \mu\text{M}$, aqueous), calculated from the $50\text{-}\mu\text{s}$ -binned time trace modulation depth, versus modulation frequency (red \blacktriangle , varied from 500 to 3900 Hz). Cy3 emission was excited with primary 496 nm cw ($500 \text{ W}/\text{cm}^2$) and 633 nm cw secondary ($10 \text{ kW}/\text{cm}^2$) lasers. Modeled dependence of the enhancement on the modulation frequency (\blacksquare) using an acceptor dark-state quantum yield of 3×10^{-4} and dark-state lifetime of $500 \mu\text{s}$.³⁷ Inset: Integrated area of the modulation frequency component in the Fourier transform of the time trace versus the modulation frequency. (B) In contrast, 6-Fam-TAMRA enhancement versus modulation frequency shows a flat response due to the much-shorter-lived excited state. Both experimental (red \blacktriangle , varied from 500 to 3900 Hz; primary 476 nm, $10 \text{ kW}/\text{cm}^2$; secondary 561 nm, $25 \text{ kW}/\text{cm}^2$) and calculated frequency responses (\blacksquare) are plotted, showing excellent agreement. The inset shows the Fourier transform amplitude versus modulation frequency. Normalized separately, the spread in data reflects the lower enhancement of 6-Fam-TAMRA relative to that of Cy3-Cy5 (panel A).

dependent modulation depth should yield a bulk measurement of acceptor dark-state decay.

Experimentally and within our rate model, enhancement resulting from Cy5 dark-state steady-state population buildup and decay was investigated for alternating single and dual laser excitation at a range of modulation frequencies. The enhancement was characterized via both the modulation depth of the observed time trace (i.e., the ratio of dual-laser excited donor fluorescence to that from primary laser excitation alone) and the amplitude at the modulation frequency in the Fourier transform of the time trace (Figure 4A, inset). A clear and steady decrease in the modulation depth (i.e., enhancement) was observed with increasing secondary laser chopping frequency. Nearing 4 kHz modulation frequency, the enhancement decreased to $\sim 10\%$, indicating that the inverse modulation frequency is approaching the time necessary to build up or relax the dark-state populations that give observed steady-state enhancements. Incorporating the time-dependent response of the steady-state populations, our FRET rate model faithfully reproduces the observed modulation-frequency-dependent modulation depth. At too high a modulation frequency, the long-lived Cy5 steady-state population cannot re-establish its limiting value, thereby decreasing modulation depth with increasing frequency. Primarily because of the dark-state decay, the observed enhancement range enables independent estimation of the dark-state lifetime. The dark-state dynamics of cyanine dyes are reported to significantly vary depending on the environment and upon conjugation to DNA.^{39,46} Close agreement between the model and the observed frequency-dependent enhancement data was obtained, however, through modeling the dark-state lifetime as being ~ 3 -fold longer than that reported for unconjugated Cy5 in methanol (Figure 4A).³⁷ Changing other experimental parameters (e.g., dark-state quantum yield, excitation rates) only shifts the enhancement curve, without affecting dynamic range. The frequency dependence of the modulation depth, therefore, appears to be an excellent gauge of acceptor dark-state decay in bulk, with the long ($\sim 500 \mu\text{s}$) lifetime again indicating that the spectrally red-shifted cis-Cy5 observed in transient absorption studies³⁷ gives rise to the modulation of the donor emission. These parameters were consistent in both

intensity-dependent (Figure 3) and modulation-frequency-dependent (Figure 4) enhancement simulations.

In contrast to the large steady-state dark-state population of Cy5 that enables higher enhancements at lower excitation intensities, the same enhancement versus modulation frequency plot for the 6-Fam-TAMRA FRET pair exhibits an essentially flat frequency response (Figure 4B). As contrast at a given modulation frequency is limited by the time to reach at least a moderate population in the dark state and the lifetime of the dark state, the relatively fast dark-state decay of TAMRA ($\sim 10 \mu\text{s}$) leads to no observable change in the measured or modeled enhancement across a wide range of secondary laser modulation frequencies (0.3–4 kHz). This flat modulation frequency response of the FRET enhancement further confirms the role of the acceptor excited state in donor modulation. For both FRET pairs, the modulated waveform is directly encoded in the fluorescence signal, and the enhancement frequency response directly reports on the lifetime and population of the acceptor excited state and its role in dynamically inhibiting FRET to directly modulate donor fluorescence (Figure 4B).

The implementation of SAFIRE with the FRET-based system should allow for the extraction of specifically targeted signals. Exciting a $1 \mu\text{M}$ Cy3-Cy5 hairpin solution with defocused primary (496 nm) and more tightly focused and modulated secondary (633 nm) excitation enabled periodic enhancement of Cy3 fluorescence via simultaneous population of the Cy5 excited state. Synchronous ccd detection recovers only the modulated Cy3 fluorescence that arises only within the focus of both lasers. Although a large fluorescent background is observed on individual images, whole image demodulation for each ccd pixel removes out-of-focus, high background fluorescence to uniquely recover the much smaller secondary laser illumination area (Figure 5). Although capable of much higher modulation frequencies (e.g., Figure 4), the secondary laser was modulated at 4 Hz to allow 10-fold faster synchronous ccd images to be recorded, triggered from the secondary laser chopping frequency. For the low excitation intensities used, the time trace of the brightest pixel within the dual laser-illuminated area shows no evident 4 Hz modulation as any modulated signal is swamped by the very high, unmodulated, out of focus background fluorescence (Figure 5C). The Fourier transform of each pixel intensity versus time reveals that the secondary laser chopping frequency was indeed encoded only on the dual

(46) Yeh, H. C.; Puleo, C. M.; Ho, Y. P.; Bailey, V. J.; Lim, T. C.; Liu, K.; Wang, T. H. *Biophys. J.* **2008**, *95*, 729–737.

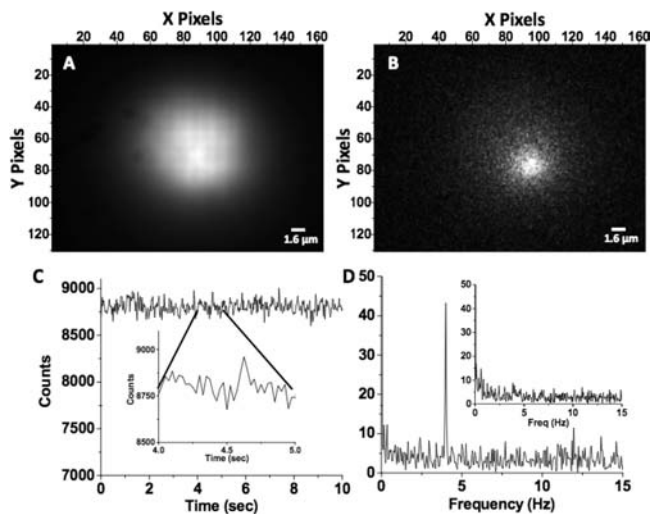


Figure 5. (A) Average frame of Cy3-Cy5 hairpin structure in solution with 496 nm cw defocused excitation (700 W/cm^2) and more tightly focused 633 nm cw laser (10 kW/cm^2). Secondary excitation was chopped at 4 Hz; synchronous ccd detection was at 40 Hz. (B) Whole image demodulation of the series of frames extracts only the modulated component, revealing pixels simultaneously exposed to both lasers. (C) Representative time trace of a pixel within the dual-illumination area. Inset showing 1-s interval of the time trace. (D) Fourier transform of the signal from panel C showing the modulation frequency encoded on the donor fluorescence and the advantage of shifting the detection frequency away from the large low frequency peak. The inset shows the Fourier transform of a single laser-illuminated pixel.

laser-illuminated fluorescent signal (Figure 5D). Demodulation of every pixel within the entire ccd image by recording the amplitude at 4 Hz recovers the image corresponding to only dual laser modulation, nearly completely removing the large background resulting from primary excitation. Although unobservable with a signal to background estimated at ~ 0.005 , the signal-to-noise within the average image is estimated in the ideal

case to be ~ 0.6 , based on the amplitude of the 4-Hz signal in the Fourier transform (Figure 5D) and the measured noise in detected pixel intensities. Upon demodulation at 4 Hz, signal (~ 41 cts) to background (~ 4 cts) improves to ~ 10 for the dual laser-illuminated pixels, while signal (41 counts) to noise (~ 1.8 counts, estimated from the standard deviation in frequency-dependent intensities) improves to 23. Demodulation thereby improves signal to background and signal-to-noise by ~ 2000 -fold and ~ 38 -fold, respectively, enabling signal detection from initially unobservable levels.

Conclusion

In conclusion we have shown that we can generally engineer optically modulated systems based on energy transfer between FRET pairs. Given the relatively short fluorescence lifetimes (a few ns) and the low probability of having simultaneous occupation of the excited state of both the donor and acceptor, reasonable enhancement can require high excitation intensities. Low intensity cw modulation, however, was readily achieved by employing a long-lived acceptor dark state with significantly shifted transient absorption to inhibit FRET (thereby dynamically increasing donor fluorescence quantum yield). In this common FRET pair, modulated fluorescence corresponding to less than 1% of total background emission was readily extracted from high background in aqueous solutions. Such large enhancement of common FRET fluorophores generalizes the optical modulation and selective detection of fluorescence through lower energy coexcitation.^{18,19} Synchronous detection (SAFIRE), then enables direct extraction of desired fluorescence from high background through selective, synchronous signal amplification.

Acknowledgment. R.M.D. gratefully acknowledges financial support from NIH R01-GM068732, and C.I.R. acknowledges NIH NRSA F31EB008324 support.

JA100175R